Journal of Molecular Liquids 425 (2025) 127276

Contents lists available at ScienceDirect

Journal of Molecular Liquids

journal homepage: www.elsevier.com/locate/molliq

Comparative analysis of drug deposition patterns among three commercial nasal spray brands: A computational and experimental study☆

Guiliang Liu [a], Mohammad Hossein Doranehgard [a,b], Xuan Ruan [b], Bingkai Chen [b], Brent Senior [c], Adam Kimple [c], Rui Ni [b], Zheng Li [a,c,*]

[a] Department of Mechatronics Engineering, Morgan State University, Baltimore, MD 21251, USA
[b] Department of Mechanical Engineering, Johns Hopkins University, Baltimore, MD 21218, USA
[c] Department of Otolaryngology/Head & Neck Surgery, University of North Carolina at Chapel Hill, USA

ARTICLE INFO

Keywords:
Nasal drug delivery
Computational fluid dynamics
Spray particle parameters
Drug deposition efficiency
Line of Sight (LOS) method

ABSTRACT

This study investigates drug deposition patterns in nasal drug delivery by combining experimental measurements with computational fluid dynamics simulations. We analyzed three, over the counter, mometasone nasal spray devices, experimentally characterizing particle diameter (dp), spray velocity (up), and spray angle (α). Unlike previous studies that relied on assumed parameters or single-brand analyses, we conducted comparative analyses using measured parameters integrated into COMSOL Multiphysics simulations. The study optimized the Line of Sight (LOS) method by exploring various spray positions and instructions to avoid anterior loss of medication in the anterior nasal cavity. Results revealed that Brand 3, with its narrow spray angle, achieved superior drug delivery efficiency when properly aligned with the target region. However, its performance decreased significantly when misaligned due to its smaller spray cone angle. Our findings show that sprays with narrower cone angles delivered medicine more effectively to the ostiomeatal complex (OMC) with up to 44% higher efficiency using the LOS method. Additionally, in cases with septal deviation, we observed a 14–20% higher drug deposition rate in the right nasal cavity compared to the left. The LOS method significantly improved drug deposition by 2.86–3 times, while the Deep Spray method further enhanced it by 38–50%. This integrated experimental-computational approach provides practical insights for optimizing nasal spray device design and administration techniques, particularly considering anatomical variations.

1. Introduction

The effective treatment of sinonasal diseases remains a significant challenge in modern medicine, partially due to the complex anatomy and limited accessibility of the sinonasal cavity [1–4]. Chronic rhinosinusitis, allergic rhinitis, and other inflammatory conditions of the paranasal sinuses affect approximately 10 % to 25 % of the population worldwide, resulting in substantial healthcare costs and decreased quality of life [5–7]. The successful management of these conditions heavily depends on the efficient delivery of therapeutic agents to the target sites within the sinonasal cavity [8–11].

Traditional drug delivery methods for treating sinus diseases, such as oral medications and nasal sprays, often face considerable limitations. Systemic administration through oral routes may lead to undesirable side effects and requires higher doses to achieve therapeutic concentrations at the target site [12,13]. Conventional nasal sprays, while more direct, frequently fail to reach the the paranasal sinuses due to the narrow anatomical passages and mucociliary clearance mechanisms that rapidly remove foreign substances from the nasal cavity [14,15].

Recent advances in drug delivery technologies have opened new avenues for enhanced therapeutic outcomes in sinonasal diseases [16]. Novel delivery systems, including nanoparticle-based carriers, mucoadhesive formulations, and targeted delivery devices, show promise in overcoming the anatomical and physiological barriers of the sinonasal cavity; however, these innovative therapeutics are not widely utilized. The most common treatment for allergic rhinitis is intranasal corticosteroids sprays but many patients do not have complete resolution of symptoms. Understanding and optimizing this simple, cost effective treatment crucial for could significantly improve symptoms in millions of patients [17–19].

☆ This article is part of a special issue entitled: 'Idrissi 60 Festschrift' published in Journal of Molecular Liquids.

* Corresponding author at: Department of Mechatronics Engineering, Morgan State University, Baltimore, MD 21251, USA.
E-mail address: Zheng.li@morgn.edu (Z. Li).

https://doi.org/10.1016/j.molliq.2025.127276
Received 24 January 2025; Received in revised form 27 February 2025; Accepted 28 February 2025
Available online 2 March 2025

Nomenclature

d_p	Particle diameter (μm)
u_p	Spray velocity (m/s)
α	Spray cone angle (°)
LOS	Line of Sight method
OMC	Ostiomeatal Complex
η	Drug delivery efficiency (%)
Re	Reynolds number (dimensionless)
ρ	Air density (kg/m^3)
μ	Dynamic viscosity of air (Pa·s)
D	Hydraulic diameter (m)
V	Volume of fluid or control volume (m^3)
CMD	Count Median Diameter (μm)
GSD	Geometric Standard Deviation (dimensionless)

The effectiveness of nasal drug delivery and ultimately efficacy is influenced by the complex structure of the nasal cavity and factors such as delivery fluid dynamics, device type, volume, and compound properties [20]. The paper reviews various methods and compounds used in managing chronic rhinosinusitis and discusses recent advancements and future directions in nasal drug delivery for upper respiratory diseases.

Werkhäuser et al. [21] investigates the efficacy and safety of Ectoin® Rhinitis Nasal Spray as a natural treatment for acute rhinosinusitis, comparing it to the commonly used Xylometazoline-containing decongestant nasal spray. Patients with acute rhinosinusitis were treated with either Ectoin® Rhinitis Spray, Xylometazoline nasal spray, or a combination of both. The study assessed rhinosinusitis symptoms, nasal oedema, and endonasal redness through rhinoscopy, and evaluated the impact on quality of life using the SNOT (Sino Nasal Outcome Test) questionnaire. Their results showed that Ectoin® Rhinitis Spray effectively reduced symptoms such as nasal obstruction, nasal secretion, facial pain/headache, and smell/taste impairment. Zhou et al. [22] evaluate the efficacy and safety of the MP-AzeFlu nasal spray, a combination of azelastine hydrochloride and fluticasone propionate, compared to the individual commercially available nasal sprays of these components in Chinese volunteers with allergic rhinitis. The research involved a clinical trial that demonstrated MP-AzeFlu's superior efficacy in alleviating nasal symptoms and improving the quality of life for patients, as compared to using azelastine or fluticasone alone. D'Angelo et al. [23] explore the use of fluorescence to evaluate the deposition and coverage of pharmaceutical formulations in the nasal tract using a silicone nasal cast and an innovative spray device. The research highlights the challenges in characterizing nasal spray deposition patterns and the importance of understanding how different formulations behave in the nasal cavity. The study employs a color-based image-analysis method to assess deposition patterns, revealing that the identity of viscosity enhancers significantly influences spray characteristics and deposition patterns.

Basu et al. [24] explore the optimization of nasal spray techniques to enhance drug delivery for sinonasal diseases. The researchers identified a novel strategy that improves drug delivery by an average of eight times compared to traditional methods, achieved by re-orienting the spray axis to utilize inertial motion of particles. This approach was developed using CFD simulations and validated with in vitro measurements in 3D-printed anatomical models. The findings suggest that this new technique could lead to personalized nasal spray instructions and improve the efficacy of nasal drug delivery, with potential implications beyond intranasal corticosteroid spray delivery. Different disease process would likely have different anatomic targets in the nose that could be optimized (i.e. targeting the olfactory cleft for olfactory disorders, the inferior turbinate for allergic rhinitis, the ethmoid bulla for sinus disease and broad distribution for vaccine delivery. Inthavong et al. [25] focus on optimizing nasal spray parameters for effective drug delivery using CFD. They utilized experimental imaging techniques, such as particle/droplet image analysis and particle image velocimetry, to identify critical parameters like particle size, spray cone diameter at break-up length, and spray cone angle. These parameters were then used to simulate particle flow within the nasal cavity using CFD, employing an Eulerian-Lagrangian scheme to track particles at a breathing rate of 10 L/min. The findings aim to guide the pharmaceutical industry in improving nasal spray device design for enhanced drug delivery efficiency. Pourmehran et al. [26] investigate the impact of inlet flow profile and nozzle diameter on drug delivery to the maxillary sinus. The research utilizes CFD to simulate and analyze how different flow profiles and nozzle sizes affect the deposition of aerosolized drugs in the sinus cavity. The findings suggest that optimizing these parameters can significantly enhance the efficiency of drug delivery, potentially improving treatment outcomes for conditions like chronic

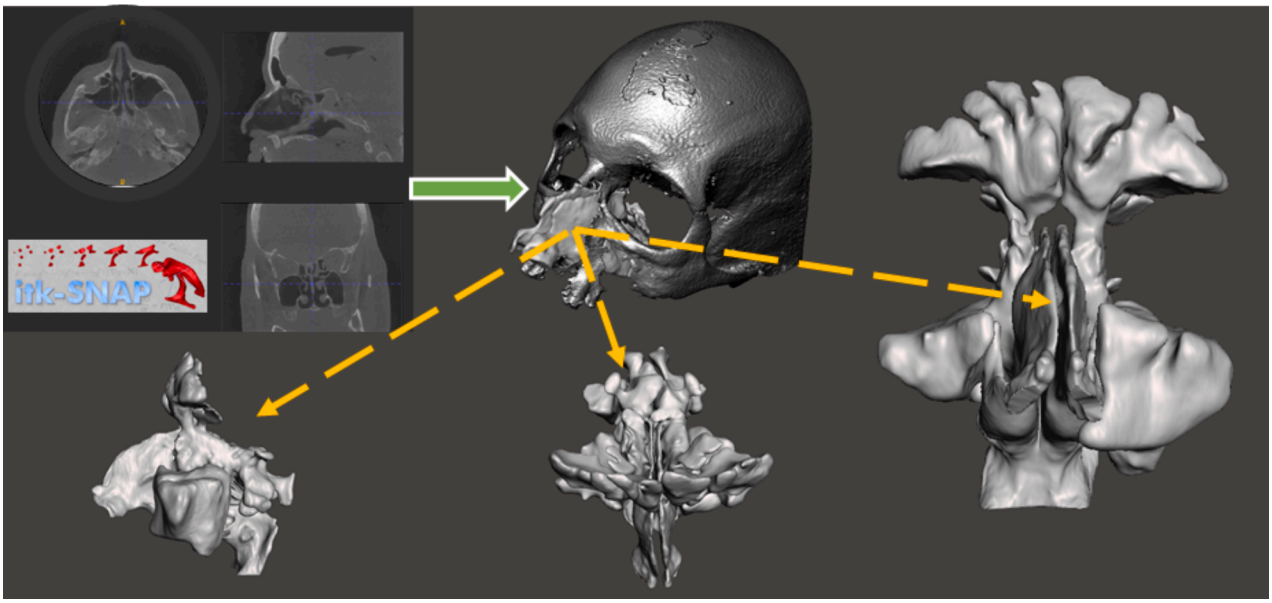

Fig. 1. Reconstruction model from CT scans using open-source software (ITK-SNAP).

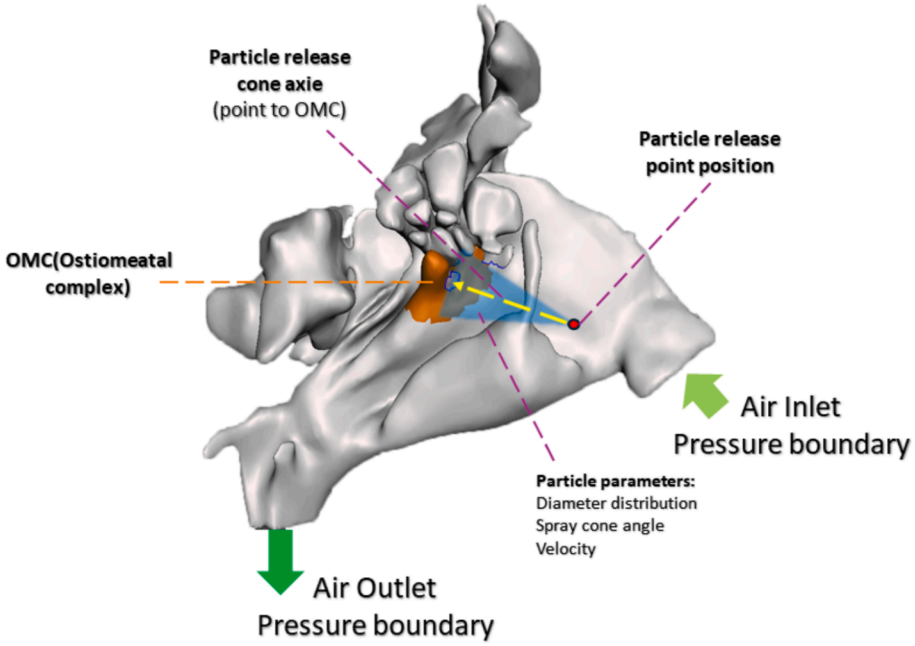

Fig. 2. The geometrical definition of the problem. The outlet was set to a −15 Pa to mimic the boundary conditions during normal human breathing, while the inlet was set to 0 Pa.

rhinosinusitis.

Despite significant advances in nasal drug delivery research, several critical gaps remain unaddressed. Most existing studies focus on single spray brands or rely on assumed particle parameters, lacking comprehensive comparative analyses based on experimental measurements. While the LOS method has demonstrated improved drug deposition efficiency, optimal spray angles and positions to avoid nasal obstructions have not been thoroughly investigate and the LOS method is a specific angle for each person's unique anatomy. Furthermore, current experimental methods, primarily using isotope tracing, provide limited resolution for accurate deposition rate measurements. The challenges are particularly pronounced for patients with deviated nasal septa, narrow internal nasal valve, where imprecise targeting can result in suboptimal drug delivery in affected nasal cavities.

In this study, we present a novel approach that addresses these limitations through a systematic investigation of three commercial nasal sprays. Our methodology combines experimental measurements of actual particle parameters with detailed computational simulations, enabling a comprehensive analysis of how particle size, velocity, and spray angle influence delivery. We extend previous research by exploring various combinations of spray positions and directions to optimize the LOS method. This integrated experimental-computational approach not only provides more accurate insights into nasal drug delivery dynamics but also offers practical guidelines for improving therapeutic outcomes in both normal and anatomically varied nasal cavities.

2. Numerical and experimental methodologies

2.1. Reconstruction model from CT scans

The computational geometric models were generated using the open-source software ITK-SNAP. As shown in Fig. 1, the nasal cavity geometry was reconstructed from CT scan data to create the three-dimensional model for numerical simulations.

2.2. CFD model and grid independent study

The geometric configuration of the physical problem is illustrated in Fig. 2. To simulate normal human breathing conditions, a pressure differential was established with the outlet maintained at −15 Pa and the inlet at atmospheric pressure (0 Pa).

Concerning the governing equations, the flow within the nasal cavity is assumed to be incompressible, laminar, isothermal, three-dimensional, and steady state. We selected the laminar flow model because previous research works [24,27–29] have shown it accurately represents airflow patterns in the nose during normal breathing conditions.

The justification for this approach is further supported by calculation of Reynolds number (Re) at the nasal inlet. Given an average nasal inlet area of 0.6 cm^2, the hydraulic diameter (D) is estimated as $D \approx 0.00874$, and assuming mean inspiratory velocity of 2 m/s, Re ($Re = \frac{\rho v D}{\mu}$) is calculated as 1118.

The calculated Re falls within the transitional regime, indicating possible localized turbulent behavior. Nevertheless, multiple studies have established that laminar flow modeling provides a valid approximation for nasal airflow during resting or moderate breathing conditions [24,27–29]. While more complex turbulence models could be employed, our study prioritizes the analysis of particle deposition patterns rather than detailed airflow characteristics. The laminar flow model offers an optimal balance between computational efficiency and accuracy in predicting particle trajectories and deposition locations, particularly since particle transport in the nasal cavity is primarily dominated by inertial impaction mechanisms.

For the described flow, we can write the continuity equation as [24,30,31]:

$$\nabla.(\vec{u}) = 0 \tag{1}$$

The 3-D velocity vector is denoted by $\vec{u}$. One can write the Navier-Stocks (momentum conservation) equations as [24,32,33]:

$$\rho(\vec{u}.\nabla)\vec{u} = -\nabla p + \mu\nabla^2\vec{u} \tag{2}$$

where, μ, ρ, and p, respectively, denotes air viscosity, pressure field and air density. It is worth mentioning that here we assume: $\rho = 1\frac{kg}{m^3}; \mu = 1.81 \times 10^{-5}\frac{kg}{m}.s$ [24]. The geometry of the nasal cavity as well as pressure difference determine the value of Re.

The Lagrangian particle tracking model is expressed as [24,34]:

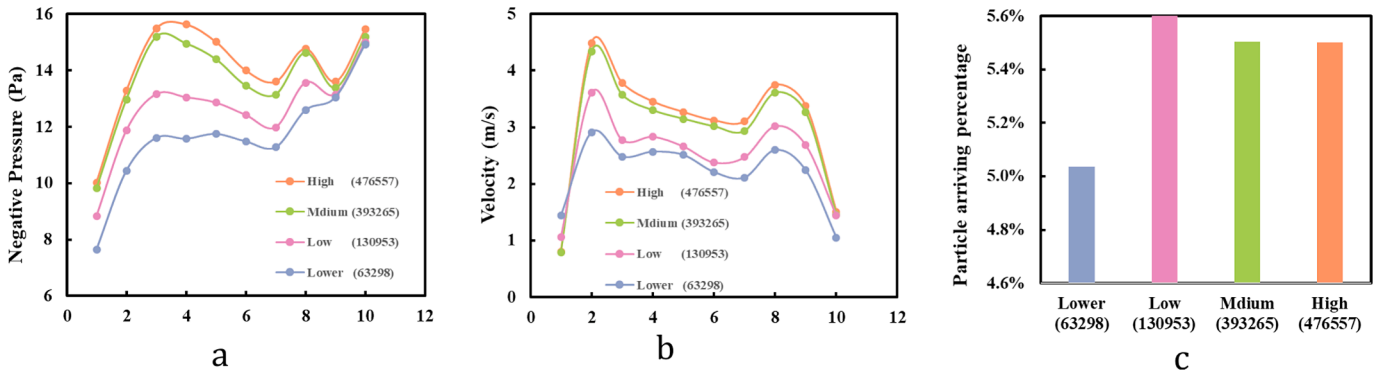

Fig. 3. Mesh indolence check study for (a) pressure (b) velocity (c) particle arriving percentage.

$$\frac{du_p}{dt} = \frac{18\mu}{d^2\rho_p}\frac{C_D Re}{24}\left(\vec{u} - \vec{u}_p\right) + \vec{g}\left(1 - \frac{\rho}{\rho_p}\right) \tag{3}$$

Here, the p subscription and d, respectively, denote particles and their diameters. While C_D shows the drag coefficient, the contribution of drag force per unit mass is given by $\frac{18\mu}{d^2\rho_p}\frac{C_D Re}{24}$. While the values of ρ, andμ are given for Eq. (2), we assume that $\vec{g} = 9.81\,\frac{m}{s^2}$ and$\rho_p = 1000\,\frac{kg}{m^3}$.

The boundary condition for particles in our computational model was configured to freeze upon surface contact, simulating the capture of drug particles by the nasal mucosal layer. This approach enables accurate quantification of drug particle arrival rates at the target region, reflecting the physiological behavior of nasal drug delivery systems. Similar boundary conditions have been successfully implemented in previous studies, such as Basu et al. [24] research work, where they employed a trap boundary condition to model drug particle adherence to airway surfaces.

Drug delivery efficiency (η) is defined as:

$$\eta = \frac{M_{target}}{M_{total}} \times 100\% \tag{4}$$

η represents the percentage of the total sprayed particle mass that successfully reaches the target region. It is a critical metric for evaluating the effectiveness of drug delivery. In this formula, the numerator is the total mass of particles reaching the target region, while the denominator is the total mass of particles emitted by the spray. Dividing these values and multiplying by 100 % yields delivery efficiency. Optimizing spray design and spray methods can improve delivery efficiency, thereby enhancing therapeutic outcomes.

This simulation demonstrates grid independence through an analysis of pressure distribution (Fig. 3a), velocity distribution (Fig. 3b), and particle arrival rates (Fig. 3c) for grid resolutions. The findings indicate that as the grid resolution increases, all parameters stabilize, with minimal changes observed at higher resolutions. This confirms that the results are no longer dependent on grid density, ensuring both their accuracy and reliability.

The drug particle deposition rates obtained in this study were

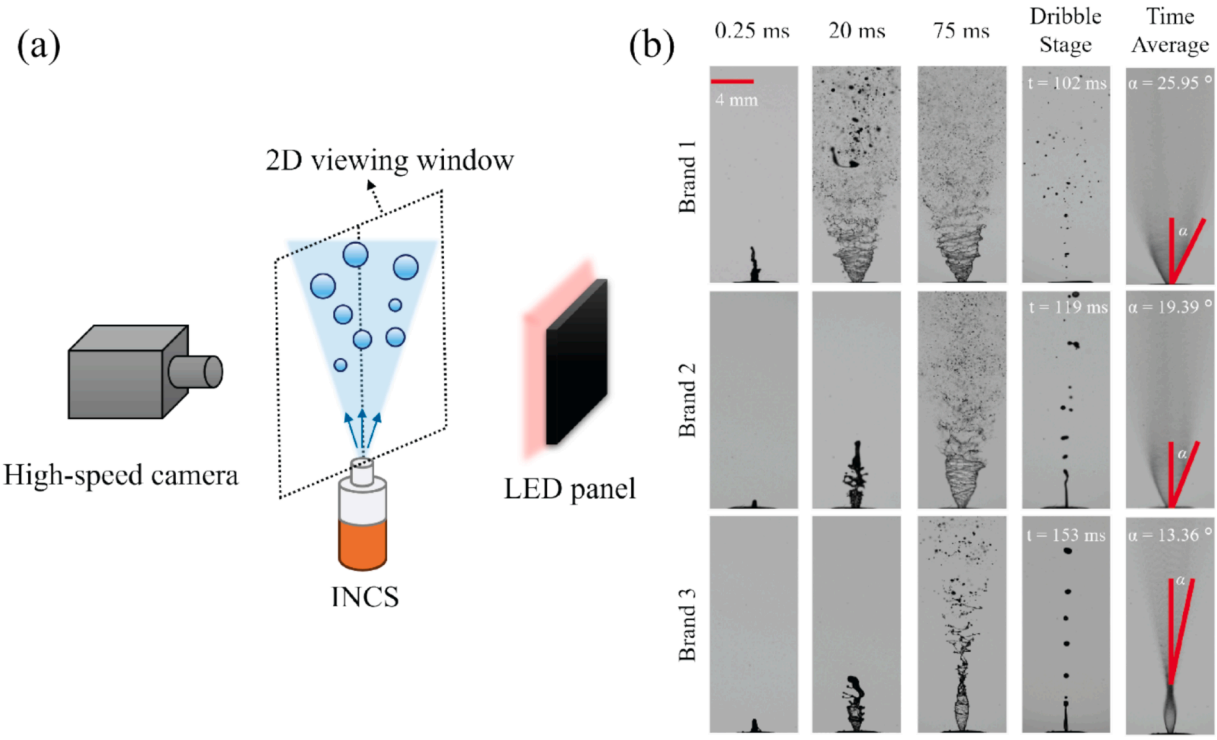

Fig. 4. (a) Schematic of the experimental system. (b) The wide variability in INCS spray development. Development stages of three commercially available INCS were captured on an optical platform at 0.25 ms, 20 ms, 75 ms and > 100 ms. Half-cone angles (α) were measured for each brand.

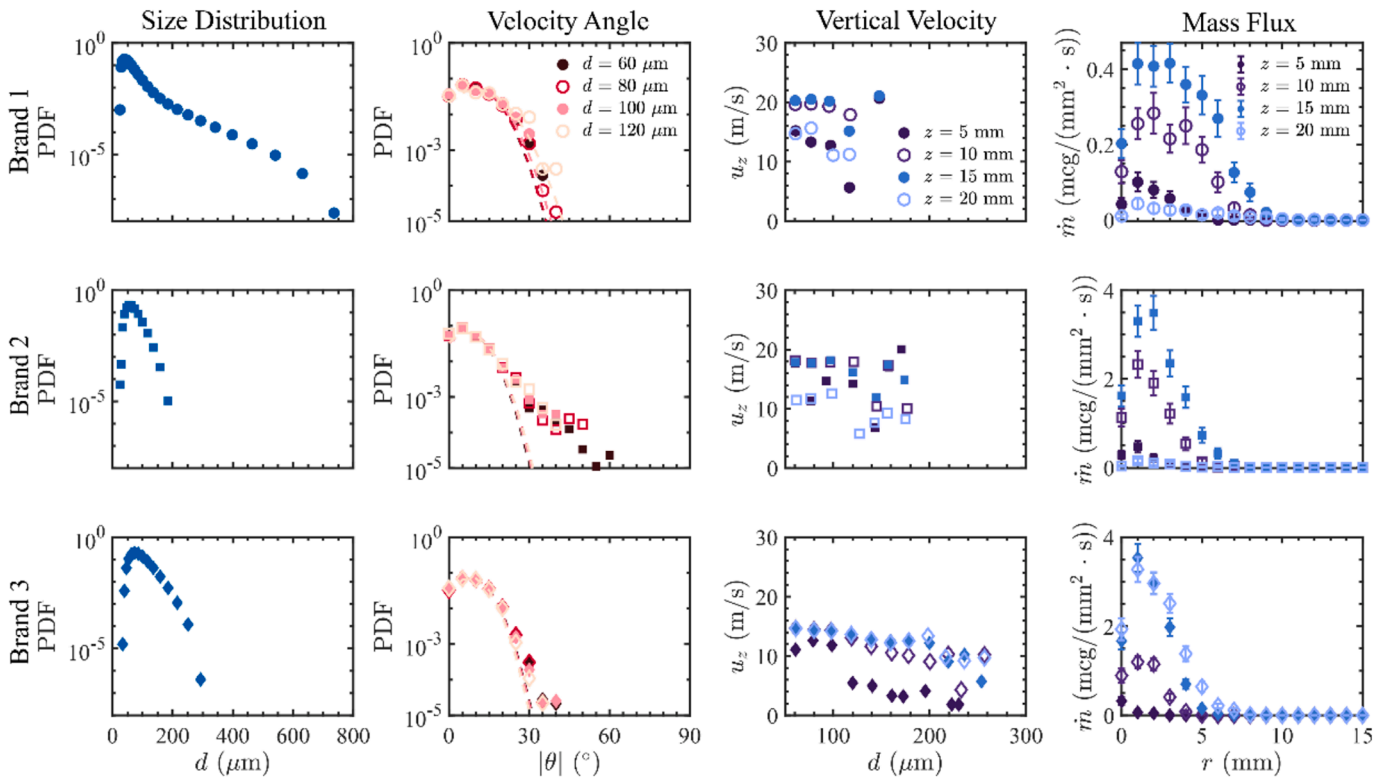

Fig. 5. Global and local characteristics of INCS. Each row represents the characteristics of each brand. The first and second columns give the PDFs of droplet sizes (d) and velocity angles (θ). The third column shows the dependence of droplet velocity (u_z) on d at different vertical positions (z), and the accelerate-then-decelerate process could be observed. The fourth column demonstrates the correlation of local mass flux $\dot{m}$ and radial position (r) at different z positions and wide variability in $\dot{m}$. The error bars represent standards deviation of $\dot{m}$ relative to the mean over time.

compared with previously reported findings in the literature. The computational results under the LOS method demonstrated good agreement with the experimental data reported by Basu et al. [24], who validated their CFD predictions using gamma scintigraphy measurements in 3D-printed anatomical replicas. Their study confirmed that well-aligned spray orientations in computational simulations accurately reflect experimental outcomes. Our LOS method findings similarly exhibited consistent drug arrival rates, further validating the reliability of our computational approach.

2.3. Experimental setups

Fig. 4 (a) illustrates the experimental setup. Each of the three intranasal corticosteroids (INCS) was mounted on an optical platform for the experiments. A diffused LED panel provided backlighting for the droplets. Following actuation, shadow images of atomized droplets were captured by a high-speed camera (Phantom v2640) equipped with a 180-mm lens (Nikon) at a frame rate of 20000 Hz. The viewing window, represented by the dashed-line area in Fig. 4 (a), is a two-dimensional plane passing through the nozzle axis just above the outlet. The window size is 29.26 × 27.88mm^2 with a resolution of 1024 × 976 pixel^2. In addition to high-speed imaging, separate tests were conducted to measure the droplet size distributions directly using a particle size analyzer (Malvern Panalytical STP5632).

After image processing, individual droplets were identified in each frame, and their trajectories were further tracked using Lagrangian particle tracking (LPT) [35]. LPT is a measurement technique that enables the tracking of individual droplet trajectories within the observation region over time. By analyzing the trajectory data, various droplet parameters were calculated, including droplet size (d), positions (r, z), radial and vertical velocities (u_r, u_z), and velocity angle (θ), defined as the angle between droplet velocity and the vertical direction.

The probability density functions (PDFs) of both d and θ were first computed to provide global statistics. To evaluate the spray performance, the viewing area was segmented into arrays of cells at fixed vertical positions (z = 5,10,15,20mm) from the nozzle tip. Each cell had a volume of 1 × 0.5 × 1.5mm^3. The local mass flux $\dot{m}(r,z)$ within each cell at (r,z) is then calculated by

$$\dot{m}(r,z) = \frac{\sum_i (\pi/6)\rho_l d_i^3 u_{z,i}}{V_c} \tag{5}$$

and averaged over time. Here ρ_l = 1000kg/m^3 is fluid density, V_c is the cell volume, d_i and $u_{z,i}$ are the diameter and the vertical velocity of the i-th droplet within the cell.

3. Results and discussions

3.1. Experimental results

Differences in spray distribution, development speed, and droplet size are observed for each INCS (Fig. 4(b)). After actuation, Brand 1 exhibit the fastest initiation, while Brand 3 is the slowest. The half-cone angle (α), defined as the angle between the outer tangent of the time averaged contour and the vertical direction, ranges from 13.36° to 25.95°, as shown in the time-averaged column in Fig. 4(b).

The size distributions shown in Fig. 5 varies widely between different brands, with ranges of 25.12 −735μm, 25.12 −184.79μm and 34.15 −292.87μm for Brand 1, 2, and 3. The most probable sizes are 39.81μm, 54.12μm and 73.56μm for Brand 1, 2 and 3 respectively.

Although comparisons between different INCS will be further explored using numerical results in later sections, it is helpful to first evaluate their performance based on the spray experiments. Previous studies have demonstrated that droplets with diameters between 20 and 120μm exhibit better nasal absorption, while larger particles are less

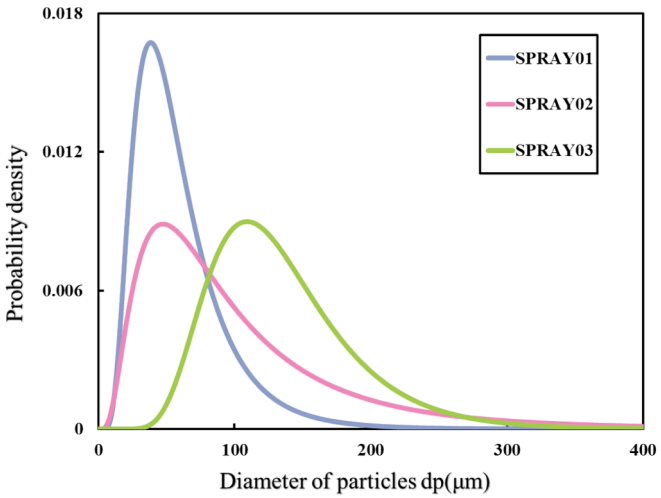

Fig. 6. Particle size distribution approximated by a lognormal distribution, based on experimental measurements.

effective [36]. We calculate the percentage of droplets generated in this effective range: Brand 1, 2 and 3 produce 98.68 %, 99.69 %, and 93.39 % of droplets within this range, respectively. The PDFs of the velocity angle (θ) for droplets in different size ranges ($60 \pm 10\mu m$, $80 \pm 10\mu m$, $100 \pm 10\mu m$, and $120 \pm 10\mu m$) are shown in the second column of Fig. 5. Substantial variations are observed in the PDFs of θ between the brands. Notably, the PDFs of $|\theta| \leq 30$ are approximately normally distributed with a non-zero mean (indicated by dash lines). For the vertical velocity u_z, droplets experience an accelerate-then-decelerate process along the vertical direction for all brands. However, Brand1 exhibits the highest droplet velocity at a given z, followed by Brand2 and then Brand3. The local mass flux $\dot{m}(r,z)$ is shown in the last column with error bars representing the standard deviations from time averaging. The mass fluxes of Brand2 and Brand3 turn out to be much higher than that of Brand1.

The spray angle is critical for the proper delivery of INCS, as inappropriate application can increase the risk of epistaxis. Given this, the cone angle is expected to play an important role, and our study demonstrates that this angle varies widely amount the three tested brands. With a narrower spray angle, droplets tend to concentrate vertically and deposit focally. While this focused delivery may be advantageous if perfectly targeted, it reduces the overall area of delivery. In Fig. 5the PDFs of θ for Brand1 and Brand3 indicate a spray pattern that is more conducive to effective broad delivery.

The vertical velocity u_z is related to $\dot{m}(r,z)$ by Eq. (5). In addition to the common accelerate-then-decelerate process along the z direction, the observation that u_z decreases with increasing droplet size d for Brand 3 arises because larger droplets are harder to accelerate, which potentially hinders their transport. This trend is also evident when comparing u_z across different brands, where a negative correlation is found between u_z and the most probable droplet size in the first column.

Finally, we quantify the total droplet mass m delivered per actuation by integrating $\dot{m}$ over time. The resulting m are 6.34mg, 25.25mg and 30.53mg for Brands 1, 2, and 3, respectively. Furthermore, m_{eff}, the mass of droplets delivered within the effective size range ($d_{\text{eff}} \leq 120\mu m$), is calculated as 6.14mg, 3.70mg and 13.93mg, respectively. This indicates that although Brand1 has a significantly lower $\dot{m}$, its effective drug delivery is improved due to higher droplet velocities within the effective size range. Furthermore, the delivery efficiency in the experiments, defined as ($\eta_{\text{exp}} = m_{\text{eff}}/m$), is calculated to be 97.61 %, 13.21 % and 44.06 % for Brands 1, 2, and 3, respectively.

Table 1
Input parameters for particle spray in the simulations.

Brand	u_z	α (cone angle °)	Lognormal distribution	
			Count Median Diameter (CMD)	Geometric Standard Deviation (GSD)
1	20.61	25.95	51.27	1.71
2	19.24	19.36	89.76	2.07
3	15.73	13.36	126.00	1.46

3.2. Implementing experimental results into COMSOL Multiphysics (numerical setup)

Concerning implementation of experimental results in our numerical setup, it should be mentioned that our primary goal is to analyze how different spray parameters affect the rate at which drug particles reach their target. To make our comparisons reasonable, we chose not to use the actual flow rates measured from different commercial sprays, as these varied considerably between brands. Instead, we took a more controlled approach: we used experimental data to create a simplified model of how spray droplets spread out, and made sure each simulation used the same number of particles. This standardized method helps us determine which spray characteristics work best for delivering particles to the target area, without confounding difference like the mass of spray. By keeping the particle count constant, we can focus purely on comparing how efficiently different spray patterns deliver medication.

The initial particle velocity was determined from experimental measurements taken at 10 mm height, where liquid atomization is complete, and velocity becomes stable. This measured velocity served as the input velocity for simulations. The spray pattern was modeled as a cone, with its angle derived from high-speed imaging data. The experimentally measured particle size distribution was simplified to a lognormal distribution to optimize computational efficiency while maintaining accurate delivery predictions. Fig. 6 shows the particle size distribution, while Table 1 lists the simulation parameters for particle sprays. The COMSOL Multiphysics model employed a lognormal distribution characterized by Count Median Diameter (CMD) and Geometric Standard Deviation (GSD), which aligned with experimental observations.

3.3. Three brands comparison based on LOS

Fig. 7a shows isolated models of the main nasal passages on both sides, with excess sinus tissue removed. The orange-highlighted region indicates the target area, OMC, which serves as the convergence point for the openings of frontal, anterior ethmoid and maxillary sinus. Effective drug delivery to this region can help alleviate sinus inflammation. Fig. 7b, c, and d depict the three spray methods employed in this study. Specifically, Fig. 7b represents the instructions recommended in the product manual for patient use [24]; Fig. 7c illustrates the LOS method proposed in previous research, wherein the nozzle is aligned directly with a notional line from the nostril to the OMC to achieve higher drug deposition. Fig. 7d demonstrates alternative combinations of nozzle insertion positions and orientations. Patients cannot directly visualize their OMC through the nostril, we extended the nozzle's insertion point more deeply and maintained its alignment toward the OMC, while avoiding anterior nasal structures that could block part of the spray. In our simulations, we evaluated a spectrum of approaches, moving from the product-manual method to the LOS method and then to this optimized nozzle-positioning technique.

In the previous section, we measured the spray characteristics—namely velocity, spray cone angle, and particle size distribution—for three commercial nasal spray products. We then applied these parameters to the LOS method for a comparative analysis. The settings for simulated particle spraying under two spray methods are

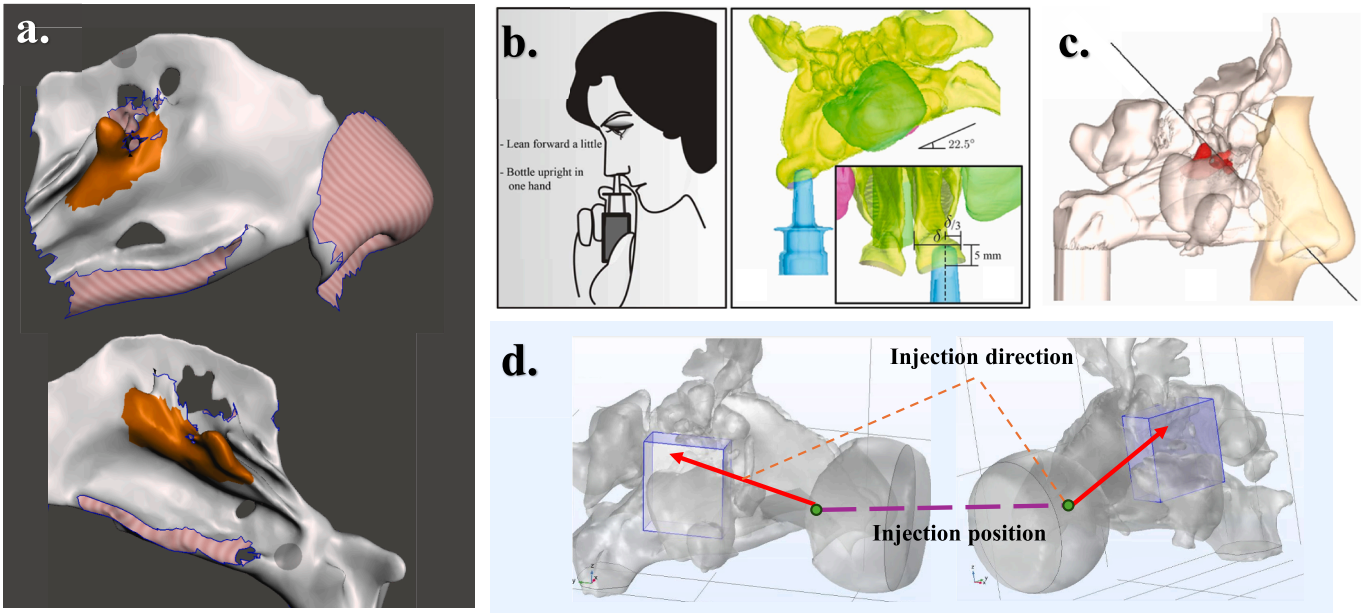

Fig. 7. Nasal passage model after sinus removal with different spray conditions: **a**: OMC (target region); **b**: Method recommended by the instructions (Original); **c**. LOS method; **d**: Deeper spray position.

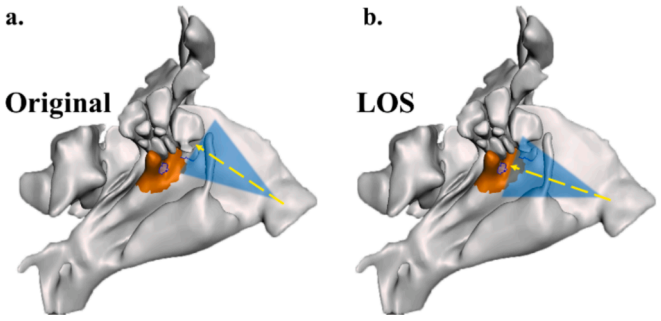

Fig. 8. Comparison of the simulation setup between the original and LOS methods a. original method b. LOS method.

compared in Fig. 8. The reconstructed model's dashed lines clearly illustrate the distinct spray directions of the two methods.

The bar charts (Fig. 9) illustrate the deposition rates of three different commercial nasal sprays administered to the left and right nasal passages using both the manufacturer-recommended method ("Original") and the LOS method. Overall, both sides exhibited significant improvement in drug deposition when using the LOS method compared to the original approach. This improvement was especially pronounced in the left nasal passage, where nasal septal deviation causes an inward curvature; under the original condition, almost all particles were intercepted by the anterior nasal tissues, resulting in near-zero deposition.

In the right nasal passage, Spray Brand 3 yielded a deposition rate of zero under the original method. This was largely due to its smaller spray cone angle—when the spray is not optimally oriented, most particles collide with anterior nasal structures. The other two sprays, benefiting from their wider cone angles, still achieved some baseline deposition under suboptimal orientation. However, once the LOS method was employed, deposition rates increased markedly for all brands, particularly for Brand 3. Its narrower cone angle allowed more particles to bypass the obstructing anterior tissues and reach the OMC once the nozzle was precisely aimed.

Fig. 10 shows the comparison between the original and LOS methods

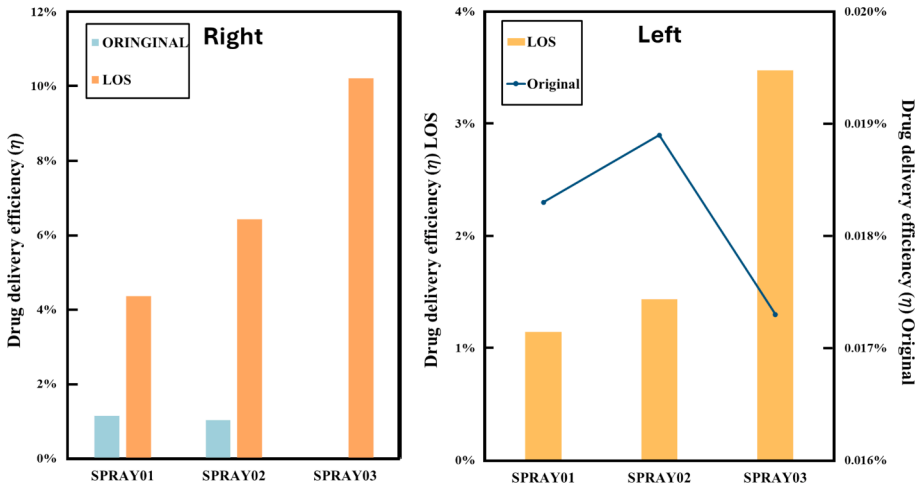

Fig. 9. Comparison of the arrival rates of three brands of spray in both nasal passages (based on the original and LOS methods).

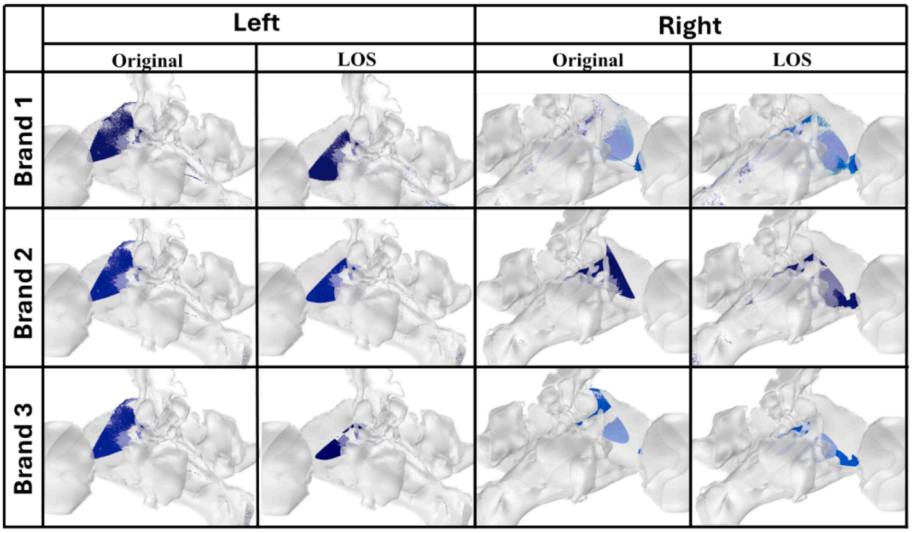

Fig. 10. Comparison of the final positions of three brands of spray particles in both nasal passages, based on the original and LOS methods.

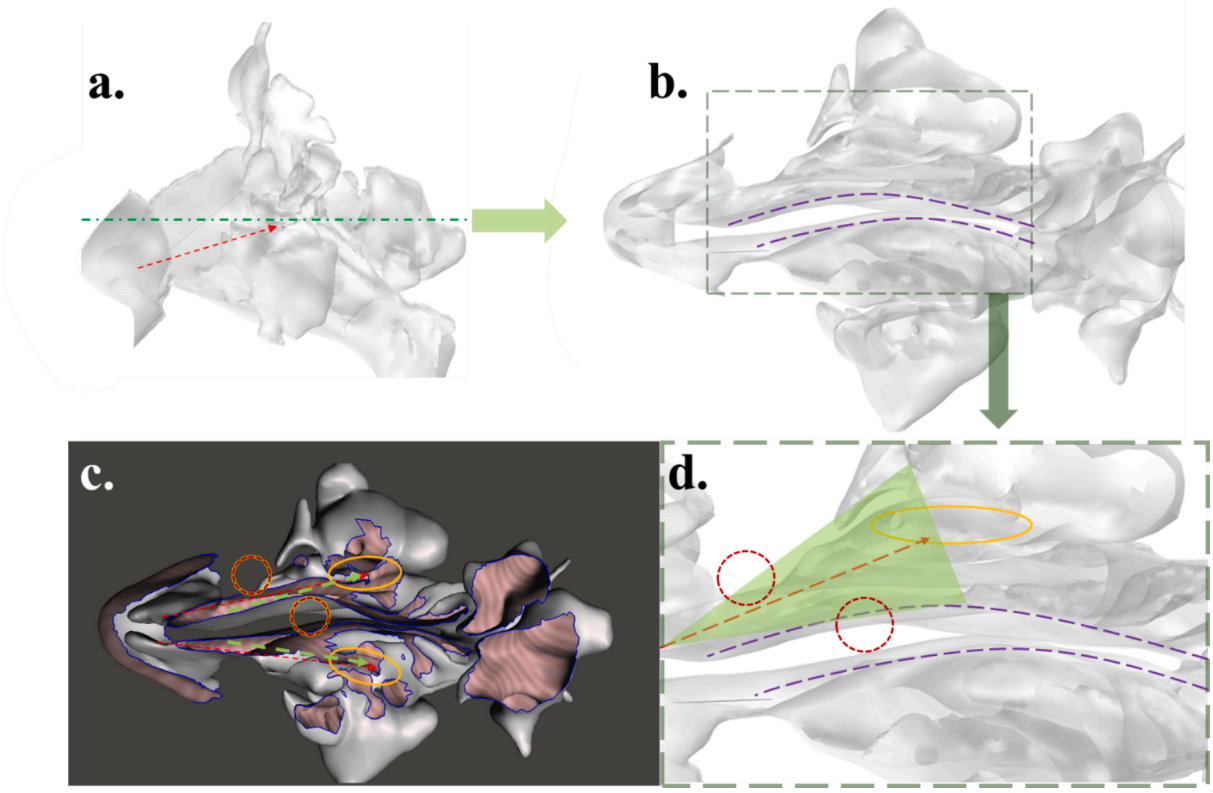

Fig. 11. A clearer drug delivery path achieved in a deviated nasal septum patient by using a deeper spray position.

for three different nasal spray brands. We can see that the LOS method among all different brands shows excel efficiency in terms of reaching droplets to the OMC.

In summary, the manufacturer's recommended instructions (Fig. 8) do not always provide high deposition rates, especially for sprays with smaller cone angles. A wider spray cone angle can ensure a baseline deposition rate even when the spray orientation is not exact. However, when precisely targeting the OMC, a smaller spray cone angle and a more centrally focused particle distribution can result in superior overall deposition.

3.4. Three brands comparison based on optimal direction

After examining multiple patient-specific nasal cavity models, we observed that for some patients it is difficult to visualize the OMC through the nostril, indicating a less discernible LOS. As shown in Fig. 11a, the patient's nasal cavity was sectioned along the green dashed line, and a top-down view of this cross-section (Fig. 11b) reveals a rightward nasal septal deviation (marked by the purple dashed line). When the magnified portion of the green dashed line is shown in Fig. 11d, two anatomical obstructions become evident in the particle trajectory, intercepting most of the sprayed particles when using a conventional LOS-based approach. Fig. 12 compares nasal spray

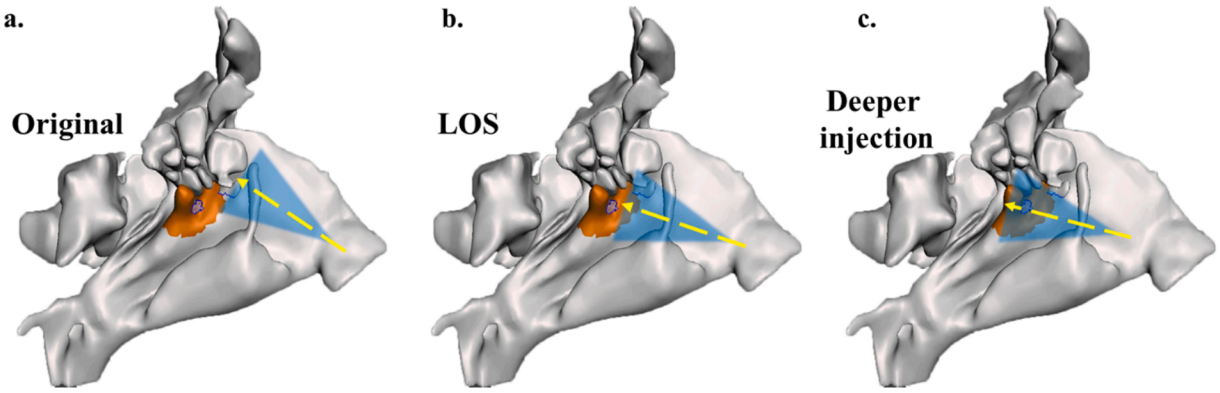

Fig. 12. Comparison of the simulation setup between original and LOS methods a. original method b. LOS method, and c. Deeper spray position (best efficiency case).

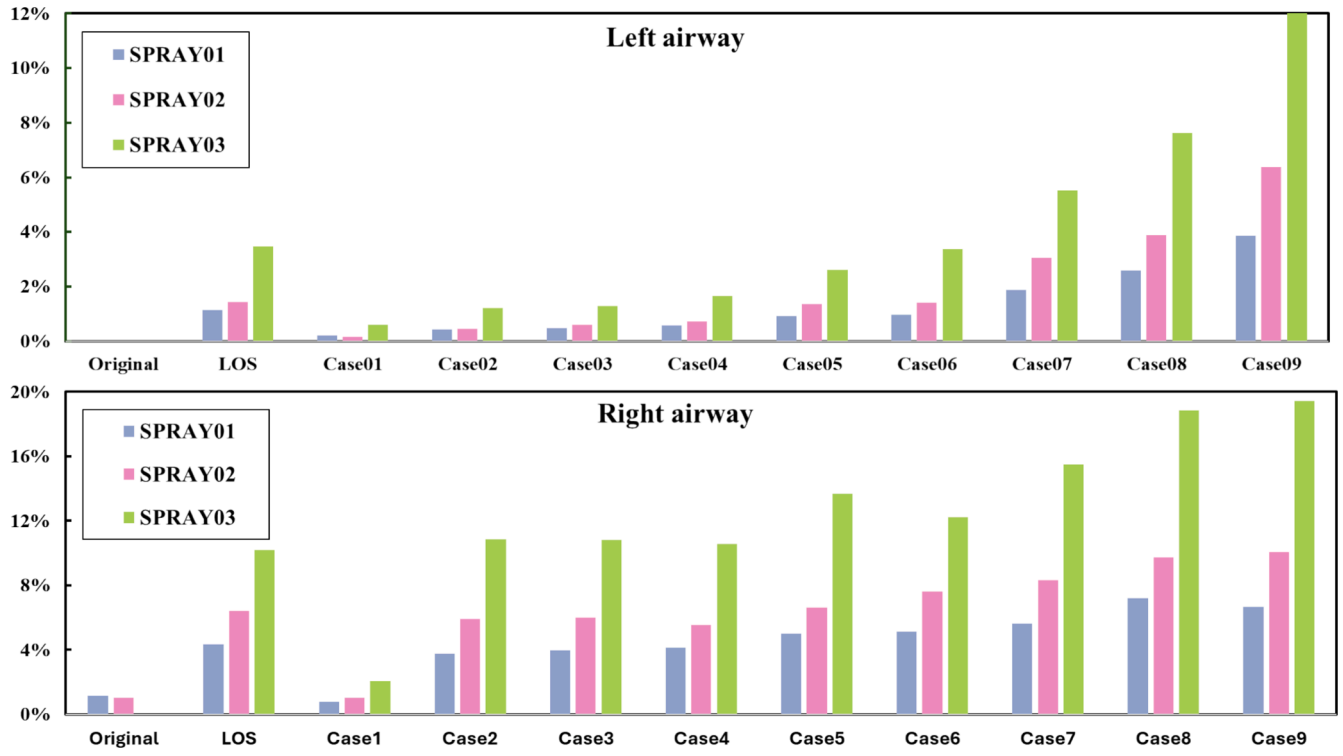

Fig. 13. Arrival rates of three spray brands under various spray conditions: a. Left nasal passage arrival rate; b. Right nasal passage arrival rate.

deposition patterns among the original method, the LOS technique, and the enhanced LOS technique with optimized insertion depth.

Nevertheless, our underlying rationale remains that aligning the spray cone axis more directly with the target region (the OMC) should yield higher deposition. To illustrate this concept, Fig. 11c demonstrates that employing a deeper spray position can render the target line clearer while avoiding anterior nasal structures that would otherwise block the spray. Based on these findings, we systematically tested multiple spray points, ranging from positions near the external naris to deeper points within the nasal passage—especially those deeper positions that provide a clearer line of sight to the OMC—to assess whether this modification would enhance drug delivery efficiency.

Fig. 13 illustrate significant differences in drug delivery efficiency between the original method and the LOS method. Under the original method, the delivery rates for all three brands are generally low, especially in the left nasal passage, where particles are almost completely blocked by anterior obstructions due to the patient's deviated nasal septum. The LOS method, which aligns the spray cone axis directly with the target region (OMC), effectively improves the delivery rate, with the most significant enhancement observed in the left nasal passage. However, as the spray points progress deeper from case 1 to case 9, the delivery rate increases further. Deeper spray points better avoid obstructions in the anterior nasal cavity, allowing particles to encounter less interference before reaching the target area. The data show that in cases 8 and 9, the delivery rates for each brand are two to three times higher than those under the LOS method, demonstrating the advantages of deeper spray points.

Additionally, the performance of different brands reflects the influence of spray cone angles and particle distribution characteristics. Brand 3, with its smaller spray cone angle, performs the best under well-aligned target-directed conditions, achieving higher delivery rates across various spray scenarios. In contrast, Brands 1 and 2, with larger spray cone angles, perform relatively better at deeper spray points but show less improvement under shallower spray conditions. This indicates that Brand 3 is more suitable for patients with complex anatomical structures under optimized targeting conditions, while other brands may

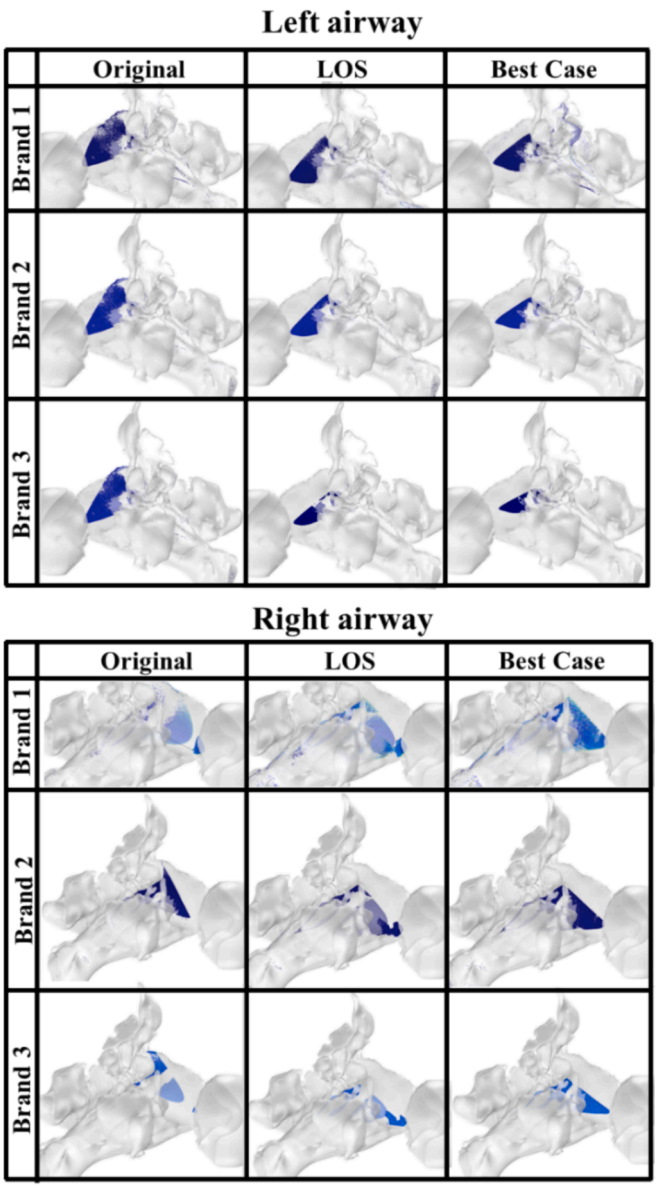

Fig. 14. Comparison of final particle positions(left and right airway)—original method, LOS method, and deeper spray method.

require additional adjustments to adapt to specific scenarios. Overall, optimizing spray positions and angles significantly enhances nasal spray drug delivery efficiency, providing valuable references for treating patients with unique anatomical structures and guiding drug design.

Fig. 14 depicts the final deposition patterns of three different commercial nasal spray brands in the left and right nasal passages under three distinct spraying conditions. By contrast, the LOS method directs substantially more particles to the intended target region (OMC). Nevertheless, many particles still impact anterior nasal structures, and a considerable fraction deposits on the middle turbinate.

In Case 9, where the nozzle is inserted more deeply, interception in the anterior portion of the nasal cavity is significantly reduced. Compared to the LOS method, this deeper placement further diminishes the area of particle deposition on the nasal vestibule. The benefit is especially pronounced for Brand 3, which has a narrower spray cone angle that allows particles to bypass anterior obstructions more effectively and reach posterior regions. Additionally, placing the nozzle deeper enables smaller particles to migrate more easily into the posterior segment of the nasal cavity.

In summary, when the spray cone axis (incidence line) is directed toward the target area, a smaller spray cone angle and a deeper incidence position can result in a higher drug particle deposition rate.

4. Conclusions

This study presents a comprehensive investigation of nasal drug delivery efficiency through a combined experimental and computational approach. By experimentally measuring particle parameters (dp, up, α) from three commercial nasal sprays and incorporating these data into COMSOL Multiphysics simulations, we established a more accurate framework for evaluating drug delivery performance. This methodology addresses the limitations of previous studies that relied on assumed parameters or single-brand analyses, providing a more realistic assessment of spray device effectiveness.

Our results demonstrate that spray parameters for over the counter medications vary considerably. These differences can alter ultimate drug delivery. Brand 3 showing superior drug delivery efficiency when properly aligned with the target region due to its minimal spray angle. However, this advantage is lost when the spray axis deviates from the optimal path or encounters anterior tissue obstruction, primarily due to its smaller spray cone angle. The comparative analysis revealed that the angle of the spray cone (how wide the spray spreads out) is a key factor in determining how well the medication reaches its target. Brand 3 performed notably better than other sprays when aimed at OMC region. This superior performance can be attributed to its narrow spray pattern – the medication particles are released in a more focused stream rather than dispersing widely. With this tighter spray cone, more particles travel directly to the intended target area instead of spreading across surrounding nasal tissues, resulting in more efficient drug delivery.

The optimization of the LOS method through various spray positions and directions has yielded valuable insights for improving nasal drug delivery techniques. These findings have important implications for both spray device design and administration protocols. Future research should focus on developing adaptive spray devices that can accommodate individual nasal cavity variations, particularly in patients with deviated septa. Additionally, the methodology established in this study provides a foundation for more detailed investigations of particle-airflow interactions and their impact on drug delivery optimization.

This study presents a thorough analysis of nasal drug deposition through combined experimental and computational approaches. However, several limitations warrant consideration. The research examines only three commercial nasal spray brands, potentially limiting the broader application of findings to other formulations or device designs. The simulations employ steady-state airflow conditions, which may not adequately represent dynamic breathing patterns or the effects of mucociliary clearance. Moreover, the study does not extensively address variations in nasal anatomy among individuals. Future research should incorporate patient-specific modeling to enhance spray delivery across different nasal structures. Finally, the experimental validation relies solely on in vitro methods, necessitating additional in vivo studies to verify the clinical significance of these results. Future investigations addressing these constraints could advance the development of personalized and efficient nasal drug delivery methods.

5. Funding support

This work is sponsored by an NSF grant with Award Number: 2401855 and a NIH grant with Award Number: R16GM153629.

CRediT authorship contribution statement

Guiliang Liu: Writing – review & editing, Writing – original draft, Visualization, Validation, Software, Methodology, Investigation, Formal analysis, Data curation, Conceptualization. **Mohammad Hossein Doranehgard:** Writing – review & editing, Writing – original draft. **Xuan**

Ruan: Writing – review & editing, Visualization, Validation, Resources, Data curation. **Bingkai Chen:** Resources, Investigation, Data curation. **Brent Senior:** Writing – review & editing, Validation, Supervision, Resources, Data curation, Conceptualization. **Adam Kimple:** Writing – review & editing, Visualization, Resources, Methodology, Investigation. **Rui Ni:** Writing – review & editing, Visualization, Validation, Resources, Methodology, Investigation, Data curation, Conceptualization. **Zheng Li:** Writing – review & editing, Writing – original draft, Visualization, Supervision, Software, Resources, Project administration, Methodology, Investigation, Funding acquisition, Formal analysis, Data curation, Conceptualization.

Declaration of competing interest

The authors declare that they have no known competing financial interests or personal relationships that could have appeared to influence the work reported in this paper.

Acknowledgment

This work is sponsored by a NSF grant with Award Number: 2401855 and a NIH grant with Award Number: R16GM153629.

Ethical approval

Deidentified human data is collected at University of North Carolina Chapel Hill (UNC) and it is transferred to Morgan State University (MSU) under the data transfer agreement between UNC and MSU.

Data availability

Data will be made available on request.

References

[1] E. De Corso, M. Rigante, D.A. Mele, S. Settimi, D. Penazzi, C. Lajolo, M. Cordaro, M. Panfili, C. Montuori, J. Galli, G. Paludetti, Real-Life Experience in the Management of Sinonasal Complications of Dental Disease or Treatments, JPM 12 (2022) 2078, https://doi.org/10.3390/jpm12122078.
[2] F. Carsuzaa, B. Verillaud, P.-Y. Marcy, P. Herman, X. Dufour, V. Favier, J. Thariat, Interdisciplinary challenges and aims of flap or graft reconstruction surgery of sinonasal cancers: What radiologists and radiation oncologists need to know, Front. Oncol. 12 (2022) 1013801, https://doi.org/10.3389/fonc.2022.1013801.
[3] D.J. Smith, E.A. Gaffney, J.R. Blake, Modelling mucociliary clearance, Respir. Physiol. Neurobiol. 163 (2008) 178–188, https://doi.org/10.1016/j.resp.2008.03.006.
[4] J. Kirch, M. Guenther, N. Doshi, U.F. Schaefer, M. Schneider, S. Mitragotri, C.-M. Lehr, Mucociliary clearance of micro- and nanoparticles is independent of size, shape and charge—an ex vivo and in silico approach, J. Control. Release 159 (2012) 128–134, https://doi.org/10.1016/j.jconrel.2011.12.015.
[5] M.S. Dykewicz, D.L. Hamilos, Rhinitis and sinusitis, J. Allergy Clin. Immunol. 125 (2010) S103–S115, https://doi.org/10.1016/j.jaci.2009.12.989.
[6] K. Avdeeva, W. Fokkens, Precision Medicine in Chronic Rhinosinusitis with Nasal Polyps, Curr. Allergy Asthma Rep. 18 (2018) 25, https://doi.org/10.1007/s11882-018-0776-8.
[7] G. De Greve, P.W. Hellings, W.J. Fokkens, B. Pugin, B. Steelant, S.F. Seys, Endotype-driven treatment in chronic upper airway diseases, Clin. Transl. Allergy 7 (2017) 22, https://doi.org/10.1186/s13601-017-0157-8.
[8] A.R. Khan, M. Liu, M.W. Khan, G. Zhai, Progress in brain targeting drug delivery system by nasal route, J. Control. Release 268 (2017) 364–389, https://doi.org/10.1016/j.jconrel.2017.09.001.
[9] C. Rollema, E.N. Van Roon, J.F.M. Van Boven, P. Hagedoorn, T. Klemmeier, J. H. Kocks, E.I. Metting, H.N.G. Oude Elberink, T.T.A. Peters, M.R.M. San Giorgi, T. W. De Vries, Pharmacology, particle deposition and drug administration techniques of intranasal corticosteroids for treating allergic rhinitis, Clin. Experimental Allergy 52 (2022) 1247–1263, https://doi.org/10.1111/cea.14212.
[10] Y. Shang, K. Inthavong, D. Qiu, N. Singh, F. He, J. Tu, Prediction of nasal spray drug absorption influenced by mucociliary clearance, PLoS One 16 (2021) e0246007, https://doi.org/10.1371/journal.pone.0246007.
[11] H. Calmet, C. Kleinstreuer, G. Houzeaux, A.V. Kolanjiyil, O. Lehmkuhl, E. Olivares, M. Vázquez, Subject-variability effects on micron particle deposition in human nasal cavities, J. Aerosol Sci. 115 (2018) 12–28, https://doi.org/10.1016/j.jaerosci.2017.10.008.
[12] S. Albu, Novel drug-delivery systems for patients with chronic rhinosinusitis, DDDT (2012) 125, https://doi.org/10.2147/DDDT.S25199.
[13] P.G. Djupesland, J.C. Messina, J.N. Palmer, Deposition of drugs in the nose and sinuses with an exhalation delivery system vs conventional nasal spray or high-volume irrigation in Draf II/III post-surgical anatomy, Rhin (2019), https://doi.org/10.4193/Rhin18.304.
[14] IIMT UNIVERSITY MEERUT (U.P), A. Gautam, D. Pathak, IIMT UNIVERSITY MEERUT (U.P), Nasal drug delivery for Chronic Rhinosinusitis: An Overview, YMER 21 (2022) 823–839. Doi: 10.37896/YMER21.07/66.
[15] W. Möller, U. Schuschnig, G. Khadem Saba, G. Meyer, B. Junge-Hülsing, M. Keller, K. Häussinger, Pulsating aerosols for drug delivery to the sinuses in healthy volunteers, Otolaryngol.–Head Neck Surg. 142 (2010) 382–388, https://doi.org/10.1016/j.otohns.2009.12.028.
[16] X. Jiang, H. Wu, A. Xiao, Y. Huang, X. Yu, L. Chang, Recent Advances in Bioelectronics for Localized Drug Delivery, Small Methods 8 (2024) 2301068, https://doi.org/10.1002/smtd.202301068.
[17] A. Alshweiat, R. Ambrus, Ii. Csóka, Intranasal Nanoparticulate Systems as Alternative Route of Drug Delivery, CMC 26 (2019) 6459–6492, https://doi.org/10.2174/0929867326666190827151741.
[18] K. Kashyap, R. Shukla, Drug Delivery and Targeting to the Brain Through Nasal Route: Mechanisms, Applications and Challenges, CDD 16 (2019) 887–901, https://doi.org/10.2174/1567201816666191029122740.
[19] J.G. Hardy, S.W. Lee, C.G. Wilson, Intranasal drug delivery by spray and drops, J. Pharm. Pharmacol. 37 (1985) 294–297, https://doi.org/10.1111/j.2042-7158.1985.tb05069.x.
[20] J. Tai, K. Lee, T.H. Kim, Current Perspective on Nasal Delivery Systems for Chronic Rhinosinusitis, Pharmaceutics 13 (2021) 246, https://doi.org/10.3390/pharmaceutics13020246.
[21] N. Werkhäuser, A. Bilstein, K. Mahlstedt, U. Sonnemann, Observational study investigating Ectoin® Rhinitis Nasal Spray as natural treatment option of acute rhinosinusitis compared to treatment with Xylometazoline, Eur. Arch. Otorhinolaryngol. 279 (2022) 1371–1381, https://doi.org/10.1007/s00405-021-06916-0.
[22] B. Zhou, L. Cheng, J. Pan, H. Wang, Y. Jin, C. Zhao, P. Lin, G. Tan, H. Fang, H. Zhang, H. Zhou, Y. Dong, H.C. Kuhl, R.K. Ramalingam, D.T. Nguyen, A Clinical Study to Assess the Efficacy and Safety of MP-AzeFlu Nasal Spray in Comparison to Commercially Available Azelastine Hydrochloride and Fluticasone Propionate Nasal Sprays in Chinese Volunteers with Allergic Rhinitis, Pulm. Ther. 9 (2023) 411–427, https://doi.org/10.1007/s41030-023-00238-8.
[23] D. D'Angelo, S. Kooij, F. Verhoeven, F. Sonvico, C. Van Rijn, Fluorescence-enabled evaluation of nasal tract deposition and coverage of pharmaceutical formulations in a silicone nasal cast using an innovative spray device, J. Adv. Res. 44 (2023) 227–232, https://doi.org/10.1016/j.jare.2022.04.011.
[24] S. Basu, L.T. Holbrook, K. Kudlaty, O. Fasanmade, J. Wu, A. Burke, B. W. Langworthy, Z. Farzal, M. Mamdani, W.D. Bennett, J.P. Fine, B.A. Senior, A. M. Zanation, C.S. Ebert, A.J. Kimple, B.D. Thorp, D.O. Frank-Ito, G.J.M. Garcia, J. S. Kimbell, Numerical evaluation of spray position for improved nasal drug delivery, Sci. Rep. 10 (2020) 10568, https://doi.org/10.1038/s41598-020-66716-0.
[25] K. Inthavong, Z.F. Tian, J.Y. Tu, W. Yang, C. Xue, Optimising nasal spray parameters for efficient drug delivery using computational fluid dynamics, Comput. Biol. Med. 38 (2008) 713–726, https://doi.org/10.1016/j.compbiomed.2008.03.008.
[26] O. Pourmehran, B. Cazzolato, Z. Tian, M. Arjomandi, The effect of inlet flow profile and nozzle diameter on drug delivery to the maxillary sinus, Biomech. Model. Mechanobiol. 21 (2022) 849–870, https://doi.org/10.1007/s10237-022-01563-8.
[27] J.S. Kimbell, S. Basu, G.J.M. Garcia, D.O. Frank-Ito, F. Lazarow, E. Su, D. Protsenko, Z. Chen, J.S. Rhee, B.J. Wong, Upper airway reconstruction using long-range optical coherence tomography: Effects of airway curvature on airflow resistance, Lasers Surg. Med. 51 (2019) 150–160, https://doi.org/10.1002/lsm.23005.
[28] J. Xi, P.W. Longest, Numerical predictions of submicrometer aerosol deposition in the nasal cavity using a novel drift flux approach, Int. J. Heat Mass Transf. 51 (2008) 5562–5577, https://doi.org/10.1016/j.ijheatmasstransfer.2008.04.037.
[29] K.T. Shanley, P. Zamankhan, G. Ahmadi, P.K. Hopke, Y.-S. Cheng, Numerical Simulations Investigating the Regional and Overall Deposition Efficiency of the Human Nasal Cavity, Inhal. Toxicol. 20 (2008) 1093–1100, https://doi.org/10.1080/08958370802130379.
[30] A. Rygg, M. Hindle, P.W. Longest, Absorption and Clearance of Pharmaceutical Aerosols in the Human Nose: Effects of Nasal Spray Suspension Particle Size and Properties, Pharm. Res. 33 (2016) 909–921, https://doi.org/10.1007/s11095-015-1837-5.
[31] Y. Shang, K. Inthavong, J. Tu, Development of a computational fluid dynamics model for mucociliary clearance in the nasal cavity, J. Biomech. 85 (2019) 74–83, https://doi.org/10.1016/j.jbiomech.2019.01.015.
[32] S. Chari, K. Sridhar, R. Walenga, C. Kleinstreuer, Computational analysis of a 3D mucociliary clearance model predicting nasal drug uptake, J. Aerosol Sci 155 (2021) 105757, https://doi.org/10.1016/j.jaerosci.2021.105757.
[33] D. Arora, K.A. Shah, M.S. Halquist, M. Sakagami, In Vitro Aqueous Fluid-Capacity-Limited Dissolution Testing of Respirable Aerosol Drug Particles Generated from Inhaler Products, Pharm. Res. 27 (2010) 786–795, https://doi.org/10.1007/s11095-010-0070-5.

[34] A. Rygg, P.W. Longest, Absorption and Clearance of Pharmaceutical Aerosols in the Human Nose: Development of a CFD Model, J. Aerosol Med. Pulm. Drug Deliv. 29 (2016) 416–431, https://doi.org/10.1089/jamp.2015.1252.
[35] N.T. Ouellette, H. Xu, E. Bodenschatz, A quantitative study of three-dimensional Lagrangian particle tracking algorithms, Exp. Fluids 40 (2006) 301–313, https://doi.org/10.1007/s00348-005-0068-7.
[36] S. Trows, K. Wuchner, R. Spycher, H. Steckel, Analytical Challenges and Regulatory Requirements for Nasal Drug Products in Europe and the U.S, Pharmaceutics 6 (2014) 195–219, https://doi.org/10.3390/pharmaceutics6020195.